Determination of Intervalley Scattering Time in Germanium by Subpicosecond Time-Resolved Raman Spectroscopy

Koichiro Tanaka, Hideyuki Ohtake,* and Tohru Suemoto
Institute for Solid State Physics, University of Tokyo, Tokyo 106, Japan
(Received 30 April 1993; revised manuscript received 29 July 1993)

Time-resolved Raman scattering measurements are made by using 110 fs laser pulses in germanium at the initial carrier density of 3×10^{18} cm^{-3}. Intensity build-up is clearly observed for the Raman scattering due to photoexcited electrons in L valleys and is quantitatively analyzed in terms of the theory on the electronic light scattering from a multicomponent electron gas. We show that photoexcited electrons initially created in the Γ valley are scattered into L valleys with a time constant of 1.2 ± 0.1 ps.

PACS numbers: 78.47.+p, 72.80.Cw, 78.30.Hv

The initial relaxation process of photoexcited carriers (electrons and holes) in femtosecond to picosecond range has been of great interest in several recent years not only in the technological domain of high speed semiconductor circuits but also in the basic research field and has been investigated by several methods: pump-probe transmission spectroscopy, up-conversion luminescence spectroscopy, and time-resolved Raman spectroscopy.

The first subpicosecond time-resolved Raman measurements were made in GaAs by Kash, Tsang, and Hvam [1]. They showed that the Raman signal of LO phonon grows gradually and has a peak value at 2 ps after excitation. Recent femtosecond measurements in GaAs under irradiation of ~ 2 eV photons revealed that electrons in the Γ valley are scattered into side valleys within 100 fs and return slowly with a time constant of ~ 2 ps [2–6]. Time-resolved Raman scattering of photoexcited electrons (electronic Raman scattering) has been measured by a single-pulse method by Kim and co-workers [2,3]. They obtained the temperature of the photoexcited electrons and showed that the cooling time of photoexcited electrons in the Γ valley is much faster than 1 ps.

In contrast to GaAs mentioned above, little has been done in germanium (Ge) concerning the fast relaxation process, though some new aspects are expected in this system, which will be useful in understanding the relaxation dynamics in semiconductors owing to some basic properties different from GaAs. The bottom of the conduction band of Ge is located in L valleys which is 0.14 eV lower than the Γ valley (indirect nature). The intervalley scattering process in this crystal has not been clarified yet, whereas electrons created in the Γ valley have a destiny of going to L valleys after a while. Time-resolved Raman measurements have been reported in Ge and decay time of nonequilibrium phonons created by the cooling process of electrons has been found to be 4 ps at room temperature [7,8]. However, time resolution of these measurements was restricted by the excitation pulse width (4 ps). There remains an unsettled question of how the photoexcited carriers relax in the very initial stage. In addition, the Fröhlich interaction does not exist in this crystal (nonpolar nature). This leads to an expectation that the relaxation process of electrons in Ge will be quite different from the situation in polar crystals, such as GaAs.

In this Letter, we report on results of the first observation of the subpicosecond time-resolved Raman scattering from photoexcited carriers in Ge under excitation above the direct gap ($E_g=0.8$ eV). We determine the intervalley scattering time from Γ valley to L valleys, and discuss the initial relaxation process of photoexcited electrons.

We used a self-mode-locked 100 fs Ti:Al_2O_3 laser system which is based on a commercial cw laser (SP3900S, Spectra Physics), modified to have two high dispersion prisms (SF-6) and a slit inside the cavity. It was pumped by an 8 W cw Ar ion laser and a typical average power was 240 mW under operation of 82 MHz at 800 nm. The spectral bandwidth of the laser is so wide (FWHM is about 110 cm^{-1}, the tail is spread over ± 150 cm^{-1}) that it is difficult to observe the electronic Raman scattering because of its small energy shift. To overcome this problem, we used a filter stage that can restrict the spectral width of the laser, keeping the transform-limit time response. In this study, we restrict the laser spectrum within ± 90 cm^{-1} as shown by arrows in Fig. 1(a). Pulse width of the laser after the filter stage measured by the autocorrelation method was 110 fs. This enables us to observe the Raman scattering down to a shift of ± 110 cm^{-1}.

In order to obtain time-resolved Raman spectra, we utilized the pump-probe method, where pump and probe pulses were set to have the same photon energy (1.52 eV) and the same average power (25 mW) with polarization perpendicular to each other. We measured three spectra under different excitation conditions: (a) only probe pulse, (b) only pump pulse, and (c) both pulses. Time-resolved spectra are obtained by a computational subtraction procedure of these spectra: (c) $-$ [(a)+(b)]. In case of the electronic Raman scattering, the obtained spectrum is interpreted as the Raman spectrum of photoexcited carriers created by the pump pulse and detected by the probe pulse delayed by t_d to the pump pulse. The pump and probe pulses are focused onto the nondoped Ge crystals having (100) surface. We denote the crystal axis of [100] direction and two equivalents as x, y, and z. The initial carrier density generated by the laser irradiation is

0031-9007/93/71(12)/1935(4)$06.00

© 1993 The American Physical Society

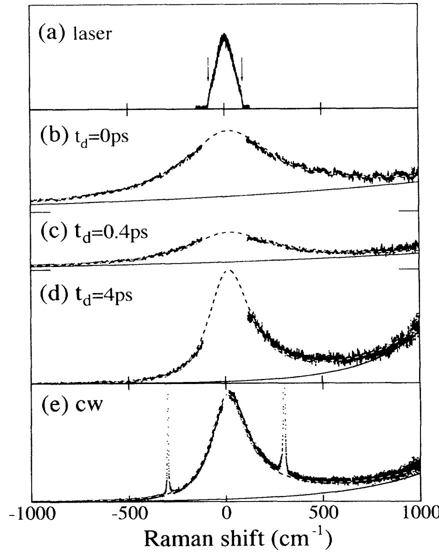

FIG. 1. Time-resolved Raman spectra of germanium at room temperature in $z(y,x)\bar{z}$ configuration at $t_d=0$ ps (b), $t_d=0.4$ ps (c), $t_d=4$ ps (d), and the ordinal Raman spectrum under steady excitation (e). The spectrum of the excitation laser (1.52 eV, 110 fs) is shown in (a). Arrows represent the limit position of the filter stage. The broken and solid curves in (b)-(e) are fitting curves described in the text. Obtained fitting parameters T_1(K), T_2(K), Γ(cm^{-1}) are (b) 2170, 2100, 260; (c) 1940, 1400, 235; (d) 420, 360, 105; (e) 415, 400, 115, respectively.

about 3×10^{18} cm^{-3} per pulse, assuming that the electron generation efficiency by one photon is unity. All measurements were made at room temperature. Secondary emission light from the sample was observed in the backscattering geometry and dispersed by a triple polychromator (DILOR) attached with a charge-coupled device camera cooled by liquid nitrogen (Princeton Instruments). The obtained spectra were corrected for the instrumental response and the ordinate scale in the figures is proportional to the photon number per unit energy interval.

Typical time-resolved spectra are shown in Fig. 1(b) ($t_d=0$ ps), Fig. 1(c) ($t_d=0.4$ ps), and Fig. 1(d) ($t_d=4$ ps) in the $z(y,x)\bar{z}$ configuration. Here, the notation "y" in the polarization configuration represents the polarization of the probe pulse. In each case, one can find a broad spectrum centered at 0 cm^{-1} and a background luminescence. The background luminescence is found to have an exponential shape as

$$I_{\rm HL}(\omega)=\exp(\hbar\omega/k_BT_1)\,, \tag{1}$$

where ω is the Raman shift (+ sign corresponds to the Stokes side). This result suggests that the luminescence is a hot luminescence which arises from the recombination of hot electrons and holes having the effective temperature T_1, as is reported in GaAs [5,6,9,10].

We found that the intensity of the broad spectra around 0 cm^{-1} increases linearly with the increase of the intensity of the pump pulse. Similar broad spectra to those shown in Figs. 1(b)-1(d) have been observed in heavily electron-doped multivalley semiconductors and assigned to the electronic Raman scattering due to excitations in an electron gas [11,12]. It is suggested that the broad spectra in Figs. 1(b)-1(d) also originate from the electronic Raman scattering due to photoexcited carriers created by the pump pulse. Following Ipatova, Subashiev, and Voitenko [13] and Klein [14], we write the spectral shape of the scattering due to excitations in a multicomponent electron gas as

$$I_{\rm ER}(\omega)=|R|^2\frac{\partial N}{\partial\mu}\left[1-\exp\left(-\frac{\hbar\omega}{k_BT_2}\right)\right]^{-1}\frac{\omega\Gamma}{\omega^2+\Gamma^2}\,, \tag{2}$$

where T_2 is the temperature of electrons which is responsible for electronic Raman scattering. In Eq. (2), Γ represents the dumping constant of electrons relevant to the light scattering, R denotes the resonance effects and the polarization selection rules, N and μ are the number of carriers and chemical potential of the system, respectively. Ipatova, Subashiev, and Voitenko derived Eq. (2) for the collision-limited electron gas in an equilibrium state of the temperature T_2, where the carrier-carrier scattering process takes place much faster than other processes (inter- and intravalley scattering by phonon emission and absorption). The theory successfully explained the electronic Raman spectra in heavily electron-doped Si [11] ($n=8\times10^{18}$-10^{20}) and Ge [12] ($n=1.6\times10^{19}$).

Application of Eq. (2) to the time-resolved electronic Raman spectra is supported by the consideration mentioned below, though it is not justified *a priori* because of the nonequilibrium nature of the hot carriers just after the ultrafast pulse excitation. In several semiconductors, such as GaAs, femtosecond luminescence and Monte Carlo simulation studies [6,9] revealed that the carrier-carrier scattering process is much faster than other processes ($\ll 100$ fs). Carriers created by the femtosecond pulses redistribute over a wide spectral range within 100 fs and are thermalized to hot Fermi distributions within 300 fs, even at excitation densities as low as 10^{17} cm^{-3}. Although Ge has a different band structure and a different crystal structure from GaAs, there should be no significant difference in the thermalization process as far as the carrier-carrier scattering is concerned: The carrier-carrier scattering rate is closely related with the carrier density, the effective mass, and the dielectric constant [9], the latter two of which are similar in GaAs and Ge. Considering current experimental conditions in Ge, the carrier density is almost 1 order larger than that in the study of GaAs, which rather makes the scattering rate large. Therefore it is quite plausible to assume that hot carriers in Ge are thermalized to hot Fermi distributions within 300 fs and Eq. (2) can be applied to the time-resolved electronic Raman scattering. As shown in Fig.

1, hot luminescence spectrum even at 0 ps, which includes the whole processes taking place within the pulse duration (~ 100 fs), has a broad spectrum spread over the wide range which includes the high energy region (< -1000 cm^{-1}) and the spectra are well described by Eq. (1). This result suggests that the carriers are thermalized to hot Fermi distributions within the pump pulse duration.

We try to fit time-resolved spectra to Eq. (3). Convolution integral is carried out for the electronic Raman component to take into account the finite spectral width of the laser

$$I(\omega) = A_1 I_{HL}(\omega) + A_2 \int_{-\infty}^{\infty} I_{ER}(\omega - v) I_{LASER}(v) dv . \quad (3)$$

Here $I_{LASER}(v)$ is the spectrum of the laser pulse, and A_1 and A_2 are arbitrary constants. Time-resolved spectra can be fitted quite excellently at any delay time as depicted in Figs. 1(b), 1(c), and 1(d) by the broken curve for total fitting and by the solid curve for the hot luminescence component.

At $t_d = 0$ ps, the spectrum of the electronic Raman scattering has a broad width and a symmetric shape. On the other hand, the spectrum at $t_d = 4$ ps has a narrower width and an asymmetric shape. This result tells us that the dumping constant Γ and the temperature T_2 decreases with increasing t_d. In Fig. 2 are shown t_d dependence of T_2 and Γ, which are determined from the curve fitting to several time-resolved spectra, by closed circles and open circles, respectively. They are fitted to phenomenological equations (4) which are shown by solid curves in the figures.

$$T_2(t) = 1700 \exp(-t/0.7) + 360 ,$$
$$\Gamma(t) = 170 \exp(-t/1.3) + 98 . \quad (4)$$

From these equations, it is found that the carriers cool down to the thermal equilibrium with lattice within a time constant of 0.7 ps and the dumping constant decreases with 1.3 ps. As for the integrated intensity of the electronic Raman component, it is noteworthy that the scattering intensity once decreases at 0.4 ps and then recovers at 4 ps (as seen in Fig. 1).

In order to identify the time-resolved spectrum at 4 ps,

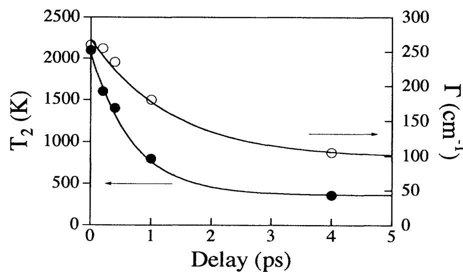

FIG. 2. Delay time dependence of T_2 (closed circles, left scale) and Γ (open circles, right scale). Solid curves are obtained by the fitting to phenomenological equations (4).

we measured electronic Raman scattering *under steady excitation conditions*. A cw $Ti{:}Al_2O_3$ laser was used with the spectral width of 0.5 cm^{-1}. The result for the $z(y,x)\bar{z}$ configuration is shown in Fig. 1(e). One can see the electronic Raman component and the hot luminescence along with LO-phonon Raman lines at ± 300 cm^{-1}. This spectrum also can be fit to Eq. (3), using the narrower laser spectrum. Obtained carrier temperature T_2 and dumping constant Γ are 400 K and 115 cm^{-1}, respectively. They are consistent with the data obtained at 300 K in n-type Ge ($n = 1.6 \times 10^{19}$) by Mestres and Cardona [12], where free electrons exist in L valleys in the steady state. Therefore, under steady excitation conditions, the origin of the electronic Raman scattering is *the electrons in L valleys* created by photoexcitation. Furthermore, one can find that the spectrum of $t_d = 4$ ps [Fig. 1(d)], is almost the same as that obtained under steady excitation [Fig. 1(e)]. *Therefore, we conclude that the origin of the electronic Raman scattering at 4 ps is photoexcited electrons in L valleys.* These results indicate that electrons initially created by the pump pulse in Γ valley are scattered into L valleys within 4 ps.

Now, we proceed to the temporal behavior of the Raman intensity. In the high temperature and dilute limit ($T > 300$, $N < 10^{19}$), $dN/d\mu$ in Eq. (2) can be rewritten as

$$\frac{\partial N}{\partial \mu} = \frac{N}{k_B T_2} . \quad (5)$$

Therefore we can estimate the number of electrons in L valleys at any delay time for the scattering intensity $I_{ER}(\omega)$ by Eq. (2). In Fig. 3(a) are shown intensities of the time-resolved spectra monitored at -115 cm^{-1} by closed circles against the delay time t_d. They are decomposed into the electronic Raman component (open circles) and the hot luminescence component (crosses). This decomposition was carried out through two processes: (1) estimate the temperature T_1 from the data simultaneously measured at large shifts in both Stokes and anti-Stokes sides, and (2) the amplitude of Raman scattering and hot luminescence contribution (A_1 and A_2) are adjusted so as to reproduce the spectral shape of the time-resolved spectra. As shown in the figure, the Raman intensity decreases rapidly from $t_d = 0$ ps and has a minimum at $t_d = 0.4$ ps and then increases gradually. After $t_d = 2$ ps, it decreases slowly. To estimate the effect of the T_2 and Γ to the Raman intensity at a fixed Raman shift, we calculated the intensity by using the second term of Eq. (3) and Eqs. (4). If N were constant in these equations, the decrease of T_2 and Γ with respect to the delay time (Fig. 2) would bring the Raman intensity at -115 cm^{-1} and would increase the delay time only by $\sim 15\%$ from 0 to 1 ps and little change after 1 ps. Therefore we can say that the change of T_2 and Γ does not influence so much the Raman intensity at -115 cm^{-1} and the main origin of the increase after 0.4 ps is the increase of the number of electrons in L valleys.

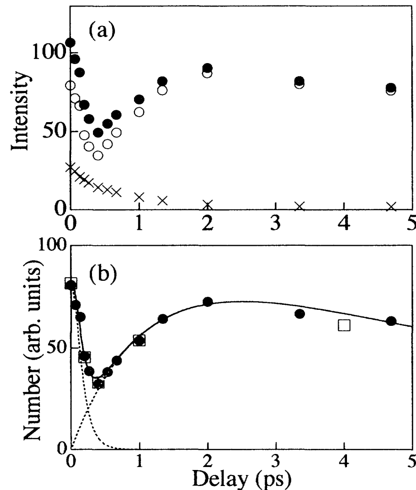

FIG. 3. (a) Time development of the Raman intensities observed at $-115\ \mathrm{cm}^{-1}$ (closed circles). Decomposed components are depicted by open circles (electronic Raman) and crosses (hot luminescence). (b) Time development of the number of carriers responsible for the electronic Raman scattering (closed circles). Open squares are the same obtained directly by the fitting of the time-resolved spectra to the Eq. (3) with Eq. (5). The solid curve is the fitting curve described in the text.

Figure 3(b) shows the time development of the number of electrons, N, responsible for the electronic Raman scattering which are calculated from the Raman intensity at $-115\ \mathrm{cm}^{-1}$ [open circles in Fig. 3(a)] and the second term of Eq. (3) with $\omega=-115$. In this case, values of T_2 and Γ are determined by the phenomenological equations (4). This analysis is justified by the agreement with data shown by open squares which are directly obtained from the spectral fitting of time-resolved spectra (parameter A_2) at several delay times. We fit the temporal change of N to a phenomenological curve which consists of two components. One is the component with an ultra fast decay (τ_1) and the other is the component with a rise (τ_2) and a slow decay (τ_3), where $\tau_1 < \tau_2 < \tau_3$. We calculated the convolution integral for the pump and probe pulses to take the finite width of the laser pulse into account. The result is shown by the solid curve in Fig. 3(b). Each component is also shown by the dotted curve in the figure. Obtained parameters, τ_1, τ_2, and τ_3 and 120 ± 50 fs, 1.2 ± 0.1 ps, and 8 ± 2 ps, respectively.

We are now ready to consider the relaxation process of photoexcited carriers. Under irradiation of 1.52 eV light, the vertical transition occurs only in the Γ valley from the heavy-hole, light-hole, and split-off-hole band and the initial electron distribution in the conduction band consists of three peaks. As is usually assumed in GaAs in the high carrier density region ($>10^{17}/\mathrm{cm}^3$), we consider a model in which electrons are quickly thermalized in the Γ valley to hot Fermi distributions by the carrier-carrier scattering [5,6,9] and then cool down by phonon emission processes (intra- and intervalley scattering). On the basis of the model, it is concluded that *the 1.2 ps rise of the carrier number is ascribed to the intervalley scattering of photoexcited electrons from the* Γ *valley to L valleys.* The time constant 1.2 ps is much longer than the value reported in GaAs [4–6,9]. This might be due to the nonpolar nature (lack of the Fröhlich interaction) of Ge which will reduce the magnitude of the electron-phonon interaction and consequently reduce the rate of the intervalley scattering.

As for the component with ultrafast decay (120 fs), one of the possible candidates for the origin is the single particle excitation in Γ valley under extreme resonant condition with the incident laser light. In this case, the decay time will be assigned to the thermalization time of electrons which localize on the dispersion curve of the conduction band in the Γ valley in the very initial stage. The long decay of 8 ps will be originated from the spatial diffusion of photoexcited carriers which has been already observed in time-resolved reflectivity measurements [8].

In summary, we made time-resolved electronic Raman measurements in Ge by 110 fs pulses. The analysis based on the thermalized multicomponent electron gas shows that photoexcited electrons initially created in the Γ valley are scattered into L valleys with a time constant of 1.2 ps.

---

*Permanent address: Department of Applied Physics, Faculty of Science, Science University of Tokyo, Tokyo 162, Japan.

[1] J. A. Kash, J. C. Tsang, and J. M. Hvam, Phys. Rev. Lett. **54**, 2151 (1985).
[2] D. Kim and P. M. Yu, Phys. Rev. B **43**, 4158 (1991).
[3] D. Kim, J. M. Jacob, J. F. Zhou, J. J. Song, H. Hou, C. W. Tu, and H. Morkoç, Phys. Rev. B **45**, 13973 (1992).
[4] J.-Y. Bigot, M. T. Portella, R. W. Schoenlein, J. E. Cunningham, and C. V. Shank, Phys. Rev. Lett. **65**, 3429 (1990).
[5] J. Shah, B. Deveaud, T. C. Damen, W. T. Tsang, A. C. Goddard, and P. Lugli, Phys. Rev. Lett. **59**, 2222 (1987).
[6] T. Elsaesser, J. Shah, L. Rota, and P. Lugli, Phys. Rev. Lett. **66**, 1757 (1991).
[7] J. F. Young, K. Wan, and H. M. van Driel, Solid State Electron. **31**, 455 (1988).
[8] A. O. Othonos, H. M. van Driel, J. F. Young, and P. J. Kelly, Phys. Rev. B **43**, 6682 (1991).
[9] L. Rota, P. Lugli, T. Elsaesser, and J. Shah, Phys. Rev. B **47**, 4226 (1993).
[10] J. C. Tsang and J. A. Kash, Phys. Rev. B **34**, 6003 (1986).
[11] G. Contreras, A. K. Sood, and M. Cardona, Phys. Rev. B **32**, 930 (1985).
[12] N. Mestres and M. Cardona, Phys. Rev. Lett. **55**, 1132 (1985).
[13] I. P. Ipatova, A. V. Subashiev, and V. A. Voitenko, Solid State Commun. **37**, 893 (1981).
[14] M. V. Klein, in *Light Scattering in Solids I*, edited by M. Cardona (Springer-Verlag, Berlin, 1983), pp. 147–204.